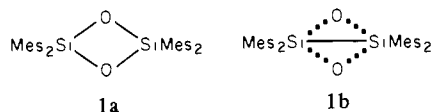


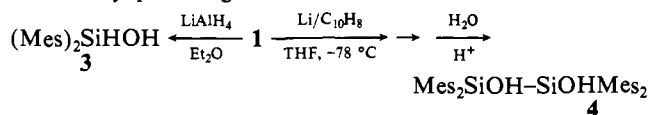
can be described as arising from a severely distorted trigonal-bipyramidal geometry about the silicons, with each silicon occupying an equatorial position of the other and the oxygens bridging adjacent apices.

The nature of bonding in the siloxane ring of **1** raises interesting questions. Two possible models will be considered: **1a**, the dia-



mond-shaped distortion in the central ring, which places the two oxygen atoms 247 pm apart and the two silicon atoms only 231 pm apart, is the result of very severe lone pair-lone pair repulsions between the oxygen atoms. This repulsion overwhelms both the nonbonded repulsion between the silicon atoms and the bond angle preferences of the ring atoms. The Si-O bonds are lengthened because of strain in the ring, as well as by O-O repulsion. **1b**, a localized two-electron bond exists between the silicon atoms, leading to the short Si-Si distance and the observed distortion of the ring, at the cost of introducing an unfavorable, very small Si-O-Si bond angle. There is a delocalized, four-center six-electron bond about the periphery of the ring, accounting for the lengthened Si-O distances. If this view is adopted, the oxygen addition reaction breaks only the π and not the σ component of the Si=Si double bond in **2**.

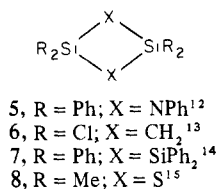
Atomic orbitals on the silicon atoms in **1** must interact strongly, but it is not yet certain if the interaction is bonding or antibonding. Detailed theoretical calculations on model compounds may be instructive.¹¹ Treatment of **1** with lithium aluminum hydride leads to **3**, the product of cleavage of the cyclodisiloxane ring. However reduction of **1** with lithium naphthalide at -78°C followed by quenching with water leads to the disilanol **4**; the



Mes = 2,4,6-trimethylphenyl

presence of a silicon-silicon bond in **4** suggests that one may likewise be present in **1**.

The isoelectronic ring systems **5-7** do not show unusual sili-



con-silicon distances, the closest being 259 pm found in **5**. The cyclodithiane **8**, however, has a planar structure with a very small Si-S-Si angle (75°), giving a silicon-silicon distance of 234 pm.¹⁶ The structure of **8** suggests that bonding between silicon and

(11) A CNDO calculation with unspecified geometry for $(\text{H}_2\text{SiO})_2$ and $(\text{Me}_2\text{SiO})_2$ showed significant Si-Si bond indices of 0.2 to 0.3 (Kirichenko, E. A.; Ermakov, A. I.; Samsonova, I. N. *Russ. J. Phys. Chem.* **1977**, *51*, 146). An MNDO calculation on $(\text{H}_2\text{SiO})_2$ suggests only a weak antibonding interaction between the silicon atoms. In addition, MNDO geometry optimization leads to a severe diamond-shaped distortion of the ring in the opposite sense from that observed, with the Si-Si distances moving to 260 pm. This result may reflect the replacement of mesityl by hydrogen in the calculation, or may be due to an inherent defect of the method.

(12) Parkanyi, L.; Dunaj-Jurco, M.; Bihatsi, L.; Hencsei, P. *Cryst. Struct. Commun.* **1980**, *9*, 1049.

(13) Vilkov, L. V.; Kusakov, M. M.; Nametkin, N. S.; Oppengeim, V. D. *Akad. Nauk SSSR Proc.* **1968**, *181*, 1038.

(14) Parkanyi, L.; Sasvari, K.; Barta, I. *Acta Crystallogr., Sect. B* **1978**, *B34*, 883.

(15) Yokoi, M.; Nomura, T.; Yamasaki, K. *J. Am. Chem. Soc.* **1955**, *77*, 4484. Yokoi, M. *Bull. Soc. Jpn.* **1957**, *30*, 1, 100.

(16) The authors of this study did not comment on this unusual silicon-silicon distance, obtained from an electron diffraction study. The precise geometry about the silicon is not known for **8** due to assumptions in the trial models.

chalcogens in other small rings might also result in penta-coordination about the silicon.

Acknowledgment. This work was supported by the Air Force Office of Scientific Research, Air Force System Command, USAF, under Grant AFOSR 82-0067, and by National Science Foundation Grant CHE-81-21122.

Supplementary Material Available: Final atomic coordinates, anisotropic thermal parameters, and selected distances and angles for **1** (3 pages). Ordering information is given on any current masthead page.

Electron Attachment to $\text{Cr}(\text{CO})_6$ at Threshold Energies[†]

J. A. Tossell,*[‡] J. H. Moore,[‡] and J. K. Olthoff[§]

*Department of Chemistry and Department of Physics
University of Maryland
College Park, Maryland 20742*

Received July 22, 1983

Using electron transmission spectroscopy¹ (ETS), we have recently shown² resonance behavior in the electron scattering cross sections from threshold to about 4 eV for $\text{Cr}(\text{CO})_6$, $\text{Mo}(\text{CO})_6$, and $\text{W}(\text{CO})_6$. The resonances observed were assigned by using bound-state multiple-scattering (MS) $X\alpha$ SCF MO calculations,³ which predicted several anion states that were either bound or within 1 eV of threshold. Recently, an ab initio restricted Hartree-Fock (RHF) SCF MO calculation⁴ on $\text{Cr}(\text{CO})_6^-$ was reported that gave as the lowest energy anion a ${}^2T_{1u}$ state, 1.54 eV above threshold. A completely new assignment of the ETS features was suggested. No other properties were reported from the RHF calculation, and no interpretation was given for the several features below 1 eV in the electron transmission spectrum. A time-of-flight mass spectrometer has recently been appended to our ETS apparatus in order to monitor anions from dissociative attachment with the same high resolution (50 meV) that characterizes the ETS experiment. Using this instrument along with new computational capabilities, we are in a position to address the question of the nature of the interaction of low-energy electrons with $\text{Cr}(\text{CO})_6$.

In Figure 1 we show the negative ion current from $\text{Cr}(\text{CO})_6$ as a function of incident electron energy. The chief features of this spectrum—a large peak near 0.5 eV with shoulders between 1 and 2 eV and between 2 and 3 eV—correspond to the prominent features of the electron transmission spectrum. The vast majority of the ions observed are $\text{Cr}(\text{CO})_5^-$ except near 1.6 eV where $\text{Cr}(\text{CO})_4^-$ contributes about 15% to the total. The production of $\text{Cr}(\text{CO})_4^-$ is clearly associated with features "B" in the electron transmission spectrum,² which we identified with processes involving the $3t_{2u}$ orbital. It is apparent that electron attachment readily occurs at energies below 1 eV, in sharp contrast to the RHF results.

In order to interpret our results we have performed continuum MS- $X\alpha$ calculations on $\text{Cr}(\text{CO})_6$ using the method described by Davenport et al.⁵ We have generated self-consistent potentials

[†] Supported by NSF CHE81-21125. From a dissertation to be submitted to the Graduate School, University of Maryland, by J. K. Olthoff in partial fulfillment of the requirements for the PhD degree in Physics.

[‡] Department of Chemistry.

[§] Department of Physics.

(1) Jordan, K. D.; Burrow, P. D. *Acc. Chem. Res.* **1978**, *11*, 344.

(2) Jordan, J. C.; Moore, J. H.; Tossell, J. A. *J. Am. Chem. Soc.* **1981**, *103*, 6632.

(3) Johnson, K. H. *Adv. Quantum Chem.* **1973**, *7*, 143.

(4) Vanquickenborne, L. G.; Verhulst, J. *J. Am. Chem. Soc.* **1983**, *105*, 1769.

(5) Davenport, J. W.; Ho, W.; Schrieffer, J. R. *Phys. Rev.* **1978**, *B17*, 3115.

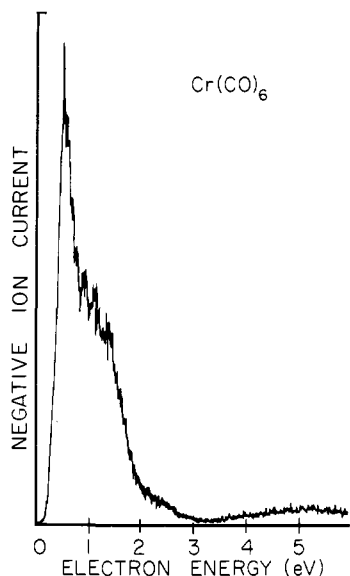


Figure 1. Ion current vs. electron impact energy on $\text{Cr}(\text{CO})_6$. The ions are essentially all $\text{Cr}(\text{CO})_5^-$.

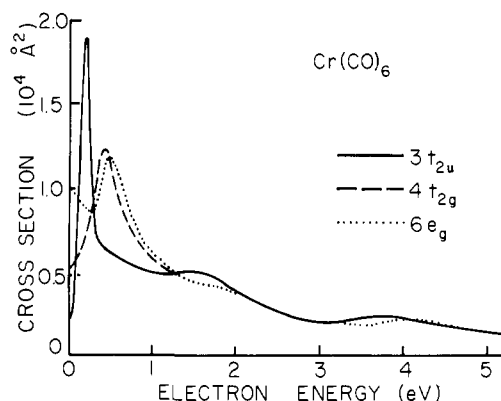


Figure 2. Calculated continuum MS-X α elastic electron scattering cross section vs. electron energy for $\text{Cr}(\text{CO})_6$ for three different potentials obtained by adding 0.5 electrons to the $3t_{2u}$, $4t_{2g}$, and $6e_g$ orbitals, respectively.

for use in the continuum calculation by adding 0.5 electrons to various empty orbitals, iterating to self-consistency, and subtracting out the effect of a stabilizing Watson sphere as described previously.² The cross sections shown in Figure 2 were determined from potentials corresponding to $3t_{2u}$, $4t_{2g}$, and $6e_g$ orbital occupations, which have calculated attachment energies of 1.7, 0.9, and 0.2 eV, respectively, within the bound-state stabilization approach.² A number of lower energy empty orbitals ($9t_{1u}$, $9a_{1g}$, $2t_{2u}$, $3t_{2g}$, and $2t_{1g}$) are predicted to generate stable anions. The calculated cross sections are similar to the experimental result, each showing maxima well below 1 eV and a shoulder between 1.2 and 2 eV. A decomposition of the cross section by the symmetry of the continuum electron for the $3t_{2u}$ potential shown in Figure 3 establishes that the low-energy maximum arises from the t_{2g} channel and the shoulder at 1.6 eV from the t_{2u} channel. The continuum MS-X α results should be considered preliminary since we have used a small basis set more appropriate for bound-state calculations and have not explored the effect of adding higher partial waves.⁶ Although the attachment energies from the bound-state calculation are in reasonable agreement with the calculated positions of the cross-section maxima, it is apparent that our previous analysis was somewhat oversimplified as evidenced by the substantial contributions in nonresonant channels and the unexpectedly low cross section in the e_g channel (also

(6) Dehmer, J. L.; Dill, D. In "Electron-Molecule and Photon-Molecule Collisions"; Rescigno, T., McKoy, V., Schneider, B., Eds.; Plenum Press: New York, 1978.

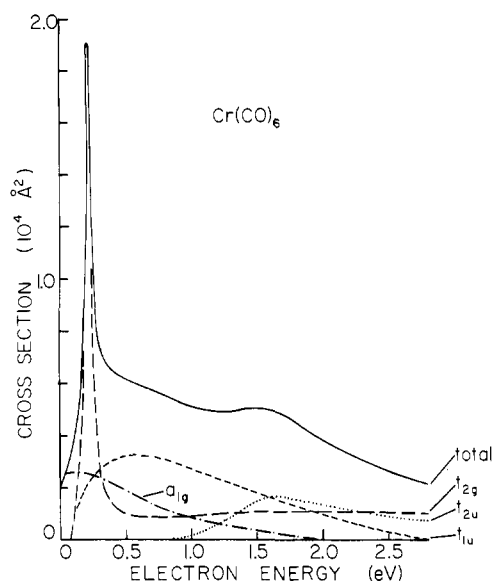


Figure 3. Decomposition of calculated cross section by symmetry of continuum electron for the scattering potential given by occupation of the $3t_{2u}$ orbital (e_g and t_{1g} channels give $\sigma < 30 \text{ \AA}^2$ and are not shown).

predicted by the RHF calculation⁴). It also appears that the RHF and MS-X α calculations give the same order of anion states but that all the states lie higher by about 2 eV in the RHF calculation. A further comparison of RHF and MS-X α results will be the subject of a later report.

Acknowledgment. Dr. J. W. Davenport (Brookhaven) kindly provided the continuum MS-X α program and advice on its use.

Registry No. $\text{Cr}(\text{CO})_6$, 13007-92-6.

(7) **Note Added in Proof:** We have recently learned of similar ion current results for $\text{Cr}(\text{CO})_6$ obtained by Pignataro et al.: Pignataro, S.; Foffari, A.; Grasso, F.; Cantone, B. *Z. Phys. Chem. (Wiesbaden)* **1965**, *47*, 106.

Electrochemical Reduction of Molybdenum(II) and Tungsten(II) Halide Cluster Ions. Electrogenerated Chemiluminescence of $\text{Mo}_6\text{Cl}_{14}^{2-}$

Daniel G. Nocera and Harry B. Gray*

Contribution No. 6890, Arthur Amos Noyes Laboratory
California Institute of Technology
Pasadena, California 91125
Received August 24, 1983

Recent work in our laboratory has revealed that the excited-state chemistry of hexanuclear molybdenum(II) and tungsten(II) halide cluster ions is unusually rich.¹⁻³ A new class of powerful inorganic oxidants ($\text{M}_6\text{X}_{14}^-$) has been identified in our electrochemical and photochemical studies, but hitherto it has not been possible to obtain reduced cluster species. Here we report experiments in which the reduced cluster $\text{Mo}_6\text{Cl}_{14}^{3-}$ has been produced cleanly, thereby making it possible to observe the electrogenerated chemiluminescence (ECL) of $\text{Mo}_6\text{Cl}_{14}^{2-}$.

Five $\text{M}_6\text{X}_{14}^{2-}$ ($\text{M} = \text{Mo}, \text{X} = \text{Cl}, \text{Br}; \text{M} = \text{W}, \text{X} = \text{Cl}, \text{Br}, \text{I}$) cluster ions were examined by cyclic voltammetry at potentials as low as -2.2 V and as high as 2.2 V vs. SCE in CH_3CN solution. All the cluster ions show irreversible oxidation waves in their cyclic voltammograms at potentials more positive than their respective

(1) Maverick, A. W.; Gray, H. B. *J. Am. Chem. Soc.* **1981**, *103*, 1298-1300.

(2) Maverick, A. W.; Najdzionek, J. S.; MacKenzie, D.; Nocera, D. G.; Gray, H. B. *J. Am. Chem. Soc.* **1983**, *105*, 1878-1882.

(3) Nocera, D. G.; Gray, H. B., manuscript in preparation.